Stability and transport of parallel velocity shear driven mode with negative magnetic shear

S. Sen, R. A. Cairns, R. G. Storer, and D. R. McCarthy

Related Articles

Additional information on Phys. Plasmas
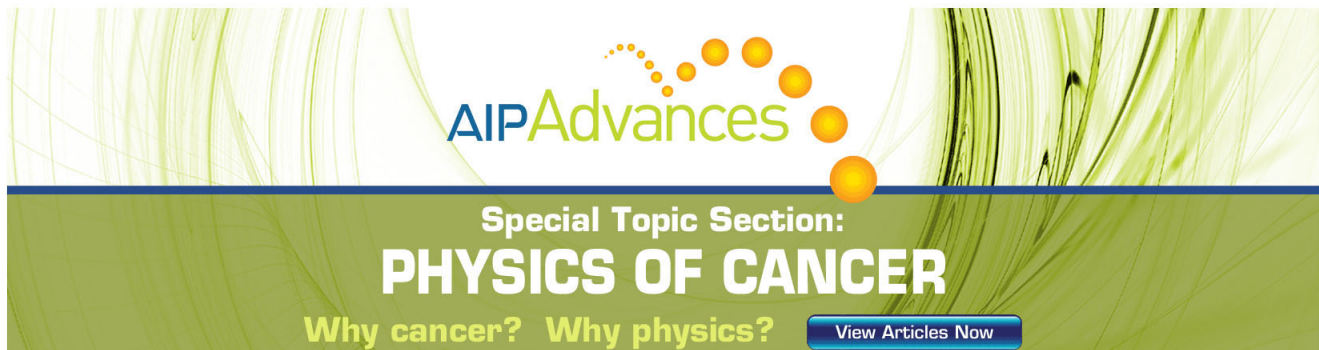
Journal Homepage: http://pop.aip.org/

Journal Information: http://pop.aip.org/about/about_the_journal

Top downloads: http://pop.aip.org/features/most_downloaded

Information for Authors: http://pop.aip.org/authors

Stability and transport of parallel velocity shear driven mode with negative magnetic shear

S. Sen

School of Mathematical and Computational Sciences, University of St. Andrews, St. Andrews, Fife KY169SS, United Kingdom and Department of Mathematics, University of North Bengal, Darjeeling 734430, India

R. A. Cairns

School of Mathematical and Computational Sciences, University of St. Andrews, St. Andrews, Fife KY16 9SS, United Kingdom

R. G. Storer

Department of Physics, The Flinders University of South Australia, GPO Box 2100, Adelaide 5001, Australia

D. R. McCarthy

Southeastern Louisiana University, Hammond, Louisiana 70402

The linear and quasilinear behavior of the drift-like perturbation with a parallel velocity shear is studied in a sheared slab geometry. Full analytic studies show that when the magnetic shear has the same sign as the second derivative of the parallel velocity with respect to the radial coordinate, the linear mode may become unstable and turbulent momentum transport increases. On the other hand, when the magnetic shear has opposite sign to the second derivative of the parallel velocity, the linear mode is completely stabilized and turbulent momentum transport reduces. © *2000 American Institute of Physics.* [S1070-664X(00)01203-9]

I. INTRODUCTION

Arguably the most remarkable story of fusion research over the past decade is the discovery of the enhanced reverse shear modes (ERS modes) in Tokamak Fusion Test Reactor (TFTR)[1] and the negative central magnetic shear modes (NCS modes) in DIII-D.[2] It is not often that a system self-organizes to a higher energy state with such a large reduction of turbulence and transport when an additional source of free energy is applied to it.[3] It is usually believed that the ERS or NCS configurations can provide the characteristics desirable for a fusion reactor.[4]

The understanding of the formation of transport barriers in the ERS or NCS plasma configurations is therefore fundamental to the development of techniques to control such barriers for tailoring profiles and for improving operating regimes further. This is especially significant because it is now widely accepted that the negative magnetic shear is not the only factor needed for the transport reduction in the ERS or NCS modes. Some of the clearest evidence comes from the comparison of the RS (reverse shear) and ERS (enhanced reverse shear) transition data in TFTR.[5] It shows that the RS phase is not necessarily an ERS phase and some other factor is needed to explain the transition. Theoretical study also indicates that the reversal of magnetic shear alone might have a little effect on the ion temperature gradient-type (ITG-type) microinstabilities.[6]

Most recently, the $\mathbf{E} \times \mathbf{B}$ shear stabilization mechanism has been proposed to explain the core transport barriers formed in plasmas with negative or reverse magnetic shear regimes.[3] It is believed that the change in the radial electric

field in the core is produced in a number of ways, for example, by toroidal flow ($v_{\phi i}$) (Ref. 7) and/or by pressure gradient (∇_{pi}) (Ref. 5) and more recently by poloidal flow ($v_{\theta i}$).[8] However, while this $\mathbf{E} \times \mathbf{B}$ shear stabilization mechanism *alone* can satisfactorily explain the confinement improvement in the edge, it may not be an obvious explanation for the core confinement improvement in the ERS and NCS plasma.[9] For example, the formation of the ERS mode in TFTR has been reported[5] at values of $\gamma_{E \times B}$ ($\mathbf{E} \times \mathbf{B}$ shearing rate), as much as a factor of 3 below γ_{max} (the maximum linear growth rate), while for the suppression of turbulence-induced transport the condition $\gamma_{E \times B} \gtrsim \gamma_{max}$ needs to be satisfied (although, this criterion of shear stabilization is only an approximate estimate). It is therefore natural that an explanation of these experimental results should be sought in the effects such optimized magnetic configurations have on microinstabilities and on the consequent transport.

In a recent important work[10] the nonlinear behavior of the parallel velocity shear (PVS) instability has been considered in a sheared slab geometry. By employing numerical procedures and by physical insight, the conclusion was drawn that when the magnetic shear has the same sign as the second derivative of the parallel velocity with respect to the radial coordinate the fluctuations grow, and the reason for this enhancement in the fluctuation level is attributed to the vortex merging that occurred in the nonlinear state. In this work, we show that the sign of the magnetic shear also strongly effects the linear growth of the mode and quasilinear transport level. When the magnetic shear has the same sign as the second derivative of the parallel flow with respect

1192

to the radial coordinate, the linear mode may become unstable and turbulent momentum transport increases. Additionally, we show when the magnetic shear has opposite sign to the second derivative of the parallel velocity, the linear mode is completely stabilized and turbulent momentum transport reduces. This result therefore shows that it is the relative sign of the second radial derivative of the equilibrium parallel flow with respect to the magnetic shear which may be the key factor for the enhanced reverse shear transition.

II. LINEAR STABILITY

We will study the short-wavelength drift-like perturbation with a parallel velocity shear. By considering the flute-like perturbations ($k_\parallel \ll k_\perp$) with a parallel velocity shear, we intend to address an additional key issue of whether the destabilization mechanism found in Ref. 10 is a general feature of all modes with structure parallel to the magnetic field. This will then allow us to investigate if the new mechanism could indeed play a role in affecting the turbulence driven by these modes and consequently will provide us with some definitive insight into its possible role in the reverse shear discharges. We adopt a two-fluid theory in a sheared slab geometry, $\mathbf{B} = B_0[\mathbf{z} + (x/L_s)\mathbf{y}]$, where L_s is the scale length of magnetic shear. The x, y, and z directions in the sheared slab geometry are defined as the radial, poloidal, and toroidal directions in the tokamak configuration. We assume a background plasma with all inhomogeneities only in the radial direction, where perturbations have the form $\phi(\mathbf{x}, t) = \phi(x)\exp[i(k_y y + k_z z - \omega t)]$. For simplicity, we take the ions to be cold and omit the electron temperature gradient. We ignore finite gyroradius effects by limiting consideration to the wavelength domain $k_\perp \rho_i \ll 1$, where ρ_i is the ion gyroradius. We then write down the linearized equations of continuity and parallel motion for the ions as[11]

$$\frac{\partial n_i}{\partial t} + \nabla_\perp \cdot [N(x)\mathbf{V}_{\perp i}] + \nabla_\parallel [(N+n)(V_{\parallel 0} + V_{\parallel i})] = 0,$$

$$m_i n_i \left[\frac{\partial V_{\parallel i}}{\partial t} + (\mathbf{V}_E + \mathbf{V}_{\parallel i}) \cdot \nabla V_{\parallel 0} \right] = -e n_i \nabla_\parallel \phi.$$

Here,

$$\nabla_\perp = i k_y \hat{e}_y + \hat{e}_x \frac{d}{dx},$$

$$\mathbf{V}_{\perp i} = \mathbf{V}_E + \mathbf{V}_{pi},$$

$$\mathbf{V}_E = -c(\nabla_\perp \phi \times \mathbf{B}_0)/B_0^2,$$

$$\mathbf{V}_{pi} = i[c(\omega - k_\parallel V_{\parallel 0}(x))/B_0 \omega_{ci}]\nabla_\perp \phi,$$

$$T_i = 0.$$

Here x is the distance from the mode rational surface defined by $\mathbf{k} \cdot \mathbf{B_0} = 0$, and $V_{\parallel 0}$ is the equilibrium parallel velocity. All other symbols are assumed to have the usual meaning unless otherwise stated explicitly. It is important to mention at this stage that in this work we make no attempt to speculate about source of these flows, although a strongly peaked ion velocity parallel to the magnetic field is observed to coexist

in tokamaks in the region where the plasma confinement is improved.[2,7,12] Parallel flow, $V_{\parallel 0}$, has therefore two effects. First, it introduces a Doppler shift, $k_\parallel V_{\parallel 0}(x)$, in all time derivatives and second, an extra term, $\mathbf{V}_E \cdot \nabla V_{\parallel 0}(x)$, representing radial convection of ion momentum. It is the second term which makes the effect of parallel flow shear completely different from that of the perpendicular flow shear.[11] We eliminate the Doppler shift by performing Galilean transformations in the $\hat{e}_\parallel$ direction. Now, using quasineutrality and the usual low-frequency and long wavelength assumptions, we obtain the radial eigenvalue equation,

$$\rho_s^2\left(\frac{d^2}{dx^2} - k_y^2\right)\phi - \left(1 - \frac{\omega_e^* + i\gamma}{\omega} + \frac{dV_{\parallel 0}}{dx} \frac{k_y \rho_s}{\omega} \frac{x}{x_s} - \frac{x^2}{x_s^2}\right)\phi = 0,$$

(1)

where

$$\rho_s^2 = \frac{C_s^2}{\omega_{ci}^2}, \quad C_s^2 = \frac{T_e}{m_i}, \quad \omega_e^*(x) = -k_y \rho_s C_s / L_n(x),$$

$$\gamma = \omega_e^* \delta, \quad x_s^2 = \frac{\omega^2}{k_\parallel'^2 C_s^2},$$

$$k_\parallel' = k_y/L_s, \quad k_\parallel = k_\parallel' x, \quad L_n(x)^{-1} = |d\ln N(x)/dx|.$$

Here, δ takes account of the dissipative effects of the electron Landau resonance and the trapped electrons, etc.

To model the equilibrium parallel velocity we assume a simple general case of the variation of $V_\parallel(x)$ with the radial distance x,

$$V_{\parallel 0}(x) = V_{\parallel 00} + V_{\parallel 0}' x + \tfrac{1}{2} V_{\parallel 0}'' x^2,$$

where

$$V_{\parallel 0}' = \frac{V_{\parallel 00}}{L_{v1}}, \quad \frac{1}{2}V_{\parallel 0}'' = \frac{V_{\parallel 00}}{L_{v2}^2},$$

where $V_{\parallel 00}$ is the velocity characterizing flow. In considering the problem with a spatial variation of $\omega_e^*(x)$, we treat the simple case in which $\omega_e^*(x)$ is to be peaked at the mode rational surface defined by $x = 0$ and has a parabolic profile: $\omega_e^*(x) \equiv \omega_0^*(1 - x^2/L_*^2)$, where L_* is the density gradient scale length and will be taken typically $\sim L_n$. This is to ensure that the mode we are investigating is located at the minimum of $(1/L_n(x))$ or at the maximum of dn/dx, which is the driving term of drift-type modes, and hence we are considering the most unstable situation. With the velocity profiles just described, Eq. (1) reduces to

$$\rho_s^2 \frac{d^2\phi}{dx^2} + (\Lambda + Px^2 - Qx)\phi = 0,$$

(2)

where

$$\Lambda = \left(\frac{\omega_0^* + i\gamma}{\omega} - k_y^2 \rho_s^2 - 1\right),$$

$$P = \left(\frac{L_n^2}{\rho_s^2 L_s^2} - 2\frac{V_{\parallel 00}}{C_s}\frac{L_n^2}{L_{v2}^2}\frac{1}{L_s \rho_s} - \frac{1}{L_*^2}\right), \quad Q = \left(\frac{V_{\parallel 00}}{C_s}\frac{L_n^2}{L_{v1}}\frac{1}{L_s \rho_s}\right).$$

In deriving Eq. (2), we have assumed the usual drift approximation, i.e., $\omega \sim \omega_0^* = k_y V_0^*$, where $V_0^* = |\rho_s C_s/L_n|$. We em-

phasize that these assumptions are made only to facilitate comparison with the experimental data and no generality whatsoever is lost thereby.

Equation (2) is a simple Weber equation. Depending on the sign of P, we have two types of solution. If $P<0$, i.e.,

$$\frac{L_n^2}{\rho_s^2 L_s^2} < 2 \frac{V_{\parallel 0}}{C_s} \frac{L_n^2}{L_{v2}^2} \frac{1}{L_s \rho_s} + \frac{1}{L_n^2}, \tag{3}$$

solution which satisfies the physical boundary condition, i.e., $\phi \rightarrow 0$ at $x = \pm \infty$ is given by

$$\phi(x) = \phi_0 \exp\left[-\frac{\sqrt{|P|}}{2\rho_s}(x - x_0)^2 \right], \tag{4}$$

where $x_0 = |Q|/2|P|$. The wave therefore does not propagate and is intrinsically undamped.

On the other hand, if $P>0$, Eq. (2) has the solution

$$\phi(x) = \phi_0 \exp\left[-i\frac{\sqrt{|P|}}{2\rho_s}(x + x_0)^2 \right]. \tag{5}$$

Thus we have now a nonlocalized mode carrying energy outward. Because of the convective wave energy leakage, the perturbation will decay in time in the absence of any energy source feeding the wave. The wave is therefore damped.

The overall stability of the mode will be determined by the strength of the driving term modeled by the $i\delta$ term and is obtained from the dispersion relation,

$$\gamma < \frac{\rho_s \left(\frac{L_n^2}{\rho_s^2 L_s^2} - 2\frac{V_{\parallel 00}}{C_s} \frac{L_n^2}{L_{v2}^2} \frac{1}{L_s \rho_s} - \frac{1}{L_n^2} \right)^{1/2} \omega_0^*}{\left(1 + k_y^2 \rho_s^2 + \frac{Q^2}{4P} \right)}. \tag{6}$$

A few interesting points emerge from relation (6). First, the sign of the flow shear has no effect on stability as it occurs through the Q^2 term in (6). It can also be concluded by noting the invariance of Eq. (2) under the combined operation of reflection $x \rightarrow -x$ and change in sign of $Q \rightarrow -Q$. Second, it is the parallel flow curvature which actually plays the key role in the stability of the mode. Velocity shear, on the other hand, shifts the potential but does not affect the quadratic structure. However, the most important observation emerging from these studies [for example, see relation (3)] is that when the magnetic shear has the same sign as the parallel flow curvature, i.e., for positive magnetic shear ($L_s > 0$), parallel flow curvature acts to destabilize the mode. This therefore shows that the increase in the level of fluctuations observed by McCarthy and Maurer,[10] when the sign of the second radial derivative of the parallel flow is the same as the magnetic shear, can possibly be explained in terms of stabilization/destabilization of the linear modes. Another important outcome of our analysis is that it shows that, as speculated by McCarthy and Maurer,[10] this mechanism of destabilization by the parallel flow curvature is a general feature of modes having a finite $k_\parallel$. However, we will later describe the fluctuations and radial transport in detail.

Now, relation (3) also allows us to make another additional important observation. We notice that for negative magnetic shear configuration ($L_s < 0$), i.e., when the magnetic shear has the opposite sign to the second derivative of the parallel flow with respect to the radial coordinate x, the parallel flow curvature acts to stabilize the mode. Flow curvature now forms an additional antiwell which pushes the wave function away from the mode rational surface, thereby enhancing stabilization. The possible role of such a magnetic configuration on the fluctuations and radial transport and its subsequent relevance to the ERS and NCS plasma will be addressed in the coming sections.

III. QUASILINEAR TRANSPORT

To see what these studies on the linear mode stability mean to the plasma transport we will now, as an example, derive analytic formulas for the quasilinear radial flux of momentum. For this we note that the general expression for the perturbed electrostatic potential is given by

$$\phi = \text{Re}\left[\sum_{k_y} \phi_0 \phi(x) \exp(ik_y y - i\omega t) \right].$$

In the representation of ϕ we use ϕ_0 to characterize the root-mean-square (rms) fluctuation level and $\phi(x)$ the normalized wave function. The $\mathbf{E} \times \mathbf{B}$ drift velocity is

$$\tilde{v}_x = -\frac{c}{B}\frac{\partial \phi}{\partial y}, \quad \tilde{v}_y = \frac{c}{B}\frac{\partial \phi}{\partial x}, \tag{7}$$

where B is the toroidal magnetic field and c is the speed of light. Now we introduce the two components of the micro Reynolds stress that measure the radial flux of the perpendicular momentum,

$$\pi_{xy} = \tilde{v}_x^* \tilde{v}_y + \tilde{v}_x \tilde{v}_y^*, \tag{8}$$

where * stands for complex conjugate. In writing Eq. (8), we leave implicit the summation over all poloidal mode numbers and all rational surfaces determined by the toroidal mode number spectra. It is straightforward to obtain the analytical expression of Eq. (8), using Eqs. (5) and (8) as follows:

$$\pi_{xy} = |\phi_0|^2 \frac{c^2}{\rho_s B^2} 2 k_y \sqrt{|P|}(x + x_0), \tag{9}$$

which at the reference mode rational surface can be simplified to

$$\pi_{xy} = |\phi_0|^2 \frac{c^2}{\rho_s B^2} k_y \frac{|Q|}{\sqrt{|P|}}. \tag{10}$$

With this simplified formula we are now in a position to see what effects the parallel flow curvature has on the radial flux with the change of its relative sign with the magnetic shear. We notice that the quantity which changes with the relative sign of the parallel flow curvature and the magnetic shear is P. Now for the normal operating phases of the tokamak operation, the relative magnitudes of the three terms in the expression of P usually are $L_n^2/\rho_s^2 L_s^2 \gg 2(V_{\parallel 00}/C_s)(L_n^2/L_{v2}^2) \times (1/L_s \rho_s) \sim 1/L_n^2$. Hence, it is clear that for the positive magnetic shear configuration ($L_s > 0$), i.e., when the magnetic shear has the same sign as the parallel flow curvature, the radial flux will grow to a larger level (due to decrease of

Phys. Plasmas, Vol. 7, No. 4, April 2000

Stability and transport of parallel velocity shear . . .

1195

TABLE I. Effect of relative sign of flow curvature and magnetic shear on radial flux.

L_s	L_{v2}	Flux
+140 cm	5 cm	0.212
+140 cm	∞	0.197
−140 cm	5 cm	0.186

TABLE II. Reduction of radial flux by varying flow curvature.

L_s	L_{v2}	Flux
−140 cm	11 cm	0.196
−140 cm	9 cm	0.194
−140 cm	7 cm	0.192
−140 cm	5 cm	0.186
−140 cm	3 cm	0.172
−140 cm	2 cm	0.150
−140 cm	1 cm	0.101

$\sqrt{P}$) than if there were no parallel flow curvature. This therefore explains the observation of McCarthy and Maurer.[10] However, our analysis also allows us to make another additional important observation. We notice from Eq. (10) that for the negative magnetic shear configuration ($L_s < 0$), i.e., when the magnetic shear has the opposite sign to the second derivative of the parallel flow, the parallel flow curvature acts to reduce the radial flux (due to increase of $\sqrt{P}$). This possibly has a crucial role in explaining the ERS and NCS discharges.

This effect is shown on a quantitative level in Table I which shows the normalized radial flux as calculated from Eq. (10) with various directions of the magnetic shear. For calculating the radial flux we have assumed $L_n \sim 10$, $L_v \sim 5$, $\rho_s \sim 0.1$ cm, and $V_{\parallel 00}/C_s \sim 1/10$. From this table, one can clearly see that when the shear is positive i.e., when the sign of the parallel flow curvature is the same as the magnetic shear, the radial flux is greater than if there were no parallel flow curvature ($L_{v2} = \infty$). On the other hand, when the shear is negative, i.e., when the sign of the parallel flow curvature is in the opposite direction of the magnetic shear, the radial flux is less than if there were no parallel flow curvature. It is important to notice that while the effect of the parallel flow curvature is robust in the case of the linear mode stability, its role in the case of radial flux is rather modest. This observation is similar to what was made in Ref. 10. This apparent disparity can be attributed to the fact that in the case of the linear mode stability, the contribution of the parallel flow curvature comes through P, whereas that in the radial flux comes through $\sqrt{P}$. Before leaving this section it is important to mention that one can similarly calculate the radial flux of the parallel momentum $\pi_{x,\parallel}$ from the equation $\pi_{x\parallel} = \tilde{v}_x^* \tilde{v}_\parallel + \tilde{v}_x \tilde{v}_\parallel^*$, where in the quasilinear approximation $\tilde{v}_\parallel = (ek_y/L_s m_i \omega)x\phi$. Proceeding as before, one can then reach a conclusion similar to that for the perpendicular counterpart.

Finally, having shown the reduction of flux for the negative magnetic shear in the preceding sections, we will now address an important question as to what extent this reduction in the radial flux can be continued by varying the scale length of the parallel flow curvature. We show this in Table II. The parameters values chosen for calculating the fluxes are the same as assumed in Table I. It is clear from Table II that, as expected, the radial flux reduces with the decrease of the scale length of the parallel flow curvature, the lower limit of which will be determined by the threshold of excitation of

the Kelvin–Helmholtz (KH) instability. However, it has been noted by Biglari et al.[13] that in order for KH to be excited, the condition $L_v(\sim L_{v2}) < L_J$ needs to be satisfied, where L_J is the width of the resistive layer and is typically a few millimeters for the DIII-D type machine. So, Table II shows that a large reduction in the radial flux is indeed possible by suitably tailoring the flow profile. Another intriguing aspect of Table II is that it also shows that as the scale length of the parallel flow curvature increases, the radial flux gradually increases before it finally reaches a state when the flux is no longer sensitive to the variation of the flow profile.

IV. CONCLUSION

In conclusion, we have identified the relative sign of the second radial derivative of the equilibrium parallel flow with respect to the magnetic shear as the key factor for the enhanced reverse shear transition. Our full analytic studies show that when the magnetic shear has the same sign as the second derivative of the parallel velocity with respect to the radial coordinate, the linear mode may become unstable and turbulent momentum transport increases. On the other hand, when the magnetic shear has an opposite sign to the second derivative of the parallel velocity, the linear mode is completely stabilized and turbulent momentum transport reduces. It is shown that a large reduction in the momentum transport is possible by suitably tailoring the parallel flow profile.

[1] F. M. Levinton et al., Phys. Rev. Lett. **75**, 4417 (1995).
[2] E. J. Strait et al., Phys. Rev. Lett. **75**, 4421 (1995).
[3] K. H. Burrell, Phys. Plasmas **4**, 1999 (1997).
[4] C. B. Forest et al., Phys. Rev. Lett. **77**, 3141 (1996).
[5] E. Mazzucato et al., Phys. Rev. Lett. **77**, 3145 (1996).
[6] S. Sen, H. Nordman, A. Sen, and J. Weiland, Phys. Scr. **56**, 86 (1997).
[7] L. L. Lao, K. H. Burrell, T. S. Casper et al., Phys. Plasmas **3**, 1951 (1996).
[8] R. E. Bell et al., Phys. Rev. Lett. **81**, 1429 (1998).
[9] S. Sen, Phys. Plasmas **5**, 1000 (1998).
[10] D. R. McCarthy and S. S. Maurer, Phys. Rev. Lett. **81**, 3399 (1998).
[11] S. Sen, M. G. Rusbridge, and R. J. Hastie, Nucl. Fusion **34**, 87 (1994).
[12] Y. Koide et al., Phys. Rev. Lett. **72**, 3662 (1994).
[13] H. Biglari, P. H. Diamond, and P. W. Terry, Phys. Plasmas B **2**, 1 (1990).